AD691506

TR69006

JANUARY

1969

© Crown Copyright 1969

ROYAL AIRCRAFT ESTABLISHMENT

TECHNICAL REPORT 69006

ENVIRONMENTAL ASSESSMENT OF THIN SILICON SOLAR CELLS FROM PILOT PRODUCTION

by

R. L. Crabb

Space Department, Royal Aircraft Establishment

D. Basnett

Electronics Department, Ferranti Limited

AUG 21 1969

DDC

UNCLASSIFIED

A

MINISTRY OF TECHNOLOGY

FARNBOROUGH HANTS

U.D.C. 629.19.066.5

ROYAL AIRCRAFT ESTABLISHMENT

Technical Report 69006

January 1969

ENVIRONMENTAL ASSESSMENT OF THIN SILICON SOLAR CELLS FROM PILOT PRODUCTION

by

R. L. Crabb

Space Department, Royal Aircraft Establishment

D. Basnett

Electronics Department, Ferranti Limited

SUMMARY

Following the earlier demonstration of the performance capabilities of 4 mil silicon solar cells and the feasibility of using these cells on large flexible arrays of space vehicles, more than a thousand 4 mil cells have been fabricated in pilot production by four routes.

The various types of cells which have been evaluated had solderless evaporated titanium-silver contacts in both a conventional and wrap-round configuration, solderless evaporated titanium-silver contacts 'over-plated' with a layer of copper-gold, and solderless plated nickel-copper-gold contacts in a conventional and wrap-round configuration. Both 1 × 2 and 2 × 2 cm, n on p cells have been manufactured from 1 and 10 ohm cm boron doped silicon. In every case, satisfactory production yields have been achieved.

The above cells have been subjected to environmental conditions aimed at studying the effects of high ambient humidity on the cell contacts during 'shelf-life' prior to launch and the degradation in performance from electron and proton irradiation encountered during long term spiral transfer orbits to synchronous altitude. Specifically the problem of low energy 'synchronous altitude' proton irradiation of exposed bar and back contacts and the protection afforded by various forms of coatings has been investigated. ( )

Paper presented at Seventh IEEE Photovoltaic Specialists' Conference, Pasadina, U.S.A., 19-21 November 1968.

Departmental Reference: Space 293

CONTENTS

1 INTRODUCTION

Increasing spacecraft power demands are continuing to be met, in the main, by silicon solar cell arrays on account of their reliability, adaptability and advanced technological status. The past few years have witnessed the design of large deployable arrays with power outputs in the multi-kilowatt range; thus the Apollo Applications Telescope Mount will embody a 4 kW cruciform array and a proposed Boeing Mars Orbiter spacecraft has been designed to incorporate a 50 kW array. The most important requirements for large solar arrays are high power-to-weight ratio and the ability to stow and support the assembly in a small volume for launching.

In an earlier paper Crabb and Treble[1] considered the theoretical implications of thinning single crystal silicon solar cells and presented results from experiments on Ferranti cells down to 4 mils (0.004 inch) thick. From this data, the power-to-weight ratio of a flexible array of 4 mil silicon cells was estimated to be 26 watts lb^{-1} at 30°C after irradiation by 10^{15} electrons cm^{-2} at 1 MeV - roughly three times that of a conventional assembly. Following this study approximately 18 months ago, it remained to be demonstrated that the more fragile thin silicon cells could be made on a production basis with acceptable yields and at a reasonable cost.

This paper presents the results of environmental studies on various thin cells, 4-6 mils thick, selected from more than 1000 thin cells fabricated in a pilot production exercise from which yield and cost factors have emerged.

The pilot production exercise was also used to provide a comparison of:

(i) Cells embodying conventional contact geometry with those embodying wrap-round contacts.

(ii) Ferranti, Ni-Cu-Au electroplated, solderless contacts - as used on Ariel 3 and Esro 2 cells - with, solderless Ti-Ag contacts similar to the standard American solderless Ti-Ag contacts, which have exhibited moisture-induced storage degradation[2] and in certain cases, found susceptible to penetration and damage by low energy (500 keV) 'synchronous altitude' protons[3].

(iii) The performance degradation of 1 and 10 ohm cm thin cells following 1 MeV electron irradiation aimed at selecting the optimum base resistivity silicon for a spacecraft's anticipated irradiation environment.

Although there have been many laboratory and orbital irradiation studies on conventional 12-16 mil silicon cells no orbital data and only limited 1 MeV electron damage data has been obtained[1] for the more radiation resistant thin n on p, 10 ohm cm cells. This information is essential for an accurate prediction of the orbital 'end-of-life' performance of a spacecraft's solar array especially for long term spiral transfer orbits to synchronous altitude. With this requirement in mind an additional objective of this Report has been to provide more extensive data on the performance degradation of thin n on p 10 ohm cm cells following irradiation by 5, 70, 100 and 140 MeV protons for fluences up to 10^{13} protons cm^{-2}.

2 THEORETICAL BACKGROUND

The predominance of indirect transitions in silicon results in photons in the red and infra-red being absorbed at an appreciable depth. For example, at a wavelength of 1 micron the absorption coefficient for silicon is 100 cm^{-1} giving a penetration depth of 100 microns. In order that the photogenerated carriers at this depth may diffuse to the shallow p-n junction and contribute to the cell output, a high base region minority carrier diffusion length is required. In fact, the base region diffusion length may be considered to be the effective thickness of the cell, any reduction in physical thickness beyond this length resulting in a loss of red response. In thin cells, there is an additional loss due to the proximity of the ohmic contact, which covers most or all of the back surface and acts as a sink for minority carriers.

An interesting feature of thin silicon cells emerges from a consideration of the effects of radiation damage. Electron or proton irradiation, such as is encountered in the Van Allen belts, produces lattice defects in the crystal, which behave intrinsically or in combination with other impurities as recombination centres. For penetrating radiation where defects are introduced uniformly throughout the volume of the solar cell the relation between base region lifetime and the parameters characterising the recombination centre is given by[4]:

$$\tau^{-1} = \tau_o^{-1} + N_r \sigma v f(E_t - E_f) \qquad (1)$$

where τ_o is the initial minority carrier lifetime

τ is the lifetime after irradiation

N_r is the density of recombination centres formed
σ is the minority carrier capture cross-section
v is the thermal velocity
$f(E_t - E_f)$ is a function related to the position of the recombination level E_t with respect to the Fermi level E_f.

Considering the case where E_f does not change during irradiation and N_r is proportional to the fluence Φ, equation (1) may be written:

$$\tau^{-1} = \tau_o^{-1} + B\,\Phi \qquad (2)$$

where B is a constant.

In terms of the diffusion length L, this becomes:

$$L^{-2} = L_o^{-2} + K\,\Phi \qquad (3)$$

where K is generally termed the 'damage coefficient'.

The half power dependence of L on 1 MeV electron fluence Φ (equation (3)) is depicted in Fig.1 in which experimental values, determined from the infra-red response of an n on p, 10 ohm cm solar cell at a wavelength of 1 micron[1], are compared with the theoretical curve for the case where L_o is 160 microns and $K = 8.89 \times 10^{-11}$ electrons^{-1}.

The degradation of base region diffusion length by radiation reduces the effective thickness of a conventional cell and results in a loss of red response similar to that brought about by physically thinning the cell. After a certain fluence, the effective thicknesses of thick and thin cells irradiated together will become equal and consequently their performances will be the same. This feature is illustrated in Fig.2 in terms of spectral response characteristics.

For low energy irradiation - e.g. low energy synchronous altitude protons - defects are no longer produced uniformly throughout the volume of the solar cell and equation (3) no longer pertains. In this case surface effects predominate; thus low energy proton irradiation of a shallow 0.2 micron solar cell p-n junction results in junction damage with an associated reduction in cell open-circuit voltage.

3 THIN CELLS

3.1 Development and pilot production

Previous development work has served to establish the range of initial and irradiated performance capability in cells ranging in thickness from 16 mils down to 4 mils and arising from this a major objective of the present work has been to investigate various techniques for producing cells 4-6 mils thick, to establish an optimum design from the standpoints of production feasibility and methods proposed for the assembly of large flexible arrays.

The proposed methods of flexible array construction require accurately size controlled cells with square edges. In addition, the assembly methods proposed require that the cell contacts should have the wrap-round configuration, both negative and positive contacts being provided on the rear surface.

Four methods for producing thin cells have been designed and investigated as follows.

Method RSC/A. This method produces either a 2 x 1 cm or 2 x 2 cm cell with square edges, in 10 ohm cm silicon 4-6 mils thick, with the contact metallised with titanium-silver in the conventional contact arrangement.

Method RSC/C. This design produced cells 4-6 mils thick, with square edges incorporating the Ferranti plated Ni-Cu-Au contact.

Method WRC/A. This design produced cells with square edges 4-6 mils thick with the titanium-silver contact system applied in the wrap-round design.

Method WRC/C. This cell design produces cells with square edges 4-6 mils thick with the Ferranti plated contact applied in a wrap-round design.

The work has consisted of designing the processes to produce the cell types and examining their production feasibility by carrying out prototype production batch exercises for each design, thus allowing a detailed examination of the working feasibility of the various production tools, jigs and techniques involved, to be made.

3.2 Titanium-silver contact metallisation

As an alternative to the Ferranti plated contact, it was decided to investigate the established American practice of evaporating titanium and silver contacts on to the cells, so that a factual comparison of these contacts in various aspects of their production and utilisation could be made.

One possible advantage of titanium-silver contacts was its use on extremely shallow diffused junctions for which the present plated schedule is difficult to control. Other interests were the relative contact strengths and corrosion resistance.

This metallisation work was essentially a two part programme firstly to establish evaporation techniques and secondly to develop and manufacture production masking jigs, capable of contacting diffused cut blanks with titanium and silver on the active surface of the cell as a continuous negative top contact bar with fingers and an isolated back contact area, both regions being isolated from the junction of the solar cell.

The work on evaporation techniques was carried out in a special vacuum equipment for metal and dielectric evaporation on solar cells. The basic technique investigation involved the evaporation of a thin barrier layer of titanium followed by a second layer of titanium and silver intermix, and finally a third layer of pure silver for electrical conduction, the whole metallising then being hydrogen sintered to give mechanical strength to the resultant metallising.

Conditions for the evaporation of titanium-silver were established which gave uniform adherent coatings with adequately hard characteristics.

3.3 Improved anti-reflective coating

Silicon monoxide as commonly employed in American cell practice and previously developed for use with Ferranti cells was found to involve output losses at the cell cover glass application stage. It was established that the reason was the non optimum refractive index of silicon monoxide as a single layer anti-reflection layer on silicon. A major effort has therefore, been expended to discover a higher refractive index film material, establish production techniques for application of the film, and confirm the physical and output characteristics of cells coated.

Trial evaporations were conducted with various materials including bismuth oxide, tantalum pentoxide, zinc sulphide, silicon nitride and ceric oxide. A programme of measurement of cell output characteristics before and after covering with microsheet covers and Silicoloid cement, based on computed short circuit current values, backed by measurements of the spectral reflectivity curves of the variously bloomed and covered cells, have been carried out.

This programme showed that by employing single layer films of ceric oxide the loss of output on cover glass application could be reduced to the range 0-2% without compromising the uncovered cell performance.

Ceric oxide is a difficult material to evaporate and control, because of its refractory nature and dissociation characteristics. However, Ferranti have developed a new form of ceric oxide evaporation system, in which $\lambda/4$ layers of ceric oxide can be applied on a production basis. It is now intended to incorporate this improved coating in all future cells used on British space projects.

In addition to developing the single layer coating of ceric oxide, various multi-layer structures involving zinc sulphide, ceric oxide and silicon monoxide were investigated in an attempt to produce more efficient blooming. With a single layer of ceric oxide, spectral reflectance curves show that average reflectance is still of the order of 7% due to the spectral reflectance curve rising on each side of reflectance minimum. It was hoped to achieve a broader based minimum region of the spectral reflectance curved by using $\lambda/4$ multi-layers of descending refractive index from the silicon interface. Unfortunately none of the combinations examined were effective, and ceric oxide is still confirmed as the optimum blooming film for silicon solar cells.

4 EXPERIMENTAL DETAILS

4.1 Performance measurements

The performance characteristics of the various types of thin cell from pilot production were measured at 30°C under filtered Xenon arc illumination set to simulate air-mass-zero sunlight (140 mW cm^{-2}) using solar cells calibrated in Malta sunlight[5], of the same type and with the same spectral response as the cells under test. The cells were electronically loaded to produce voltage-current characteristics, traced with an X-Y plotter.

Since the environmental studies described in this Report invariably involved small sequential changes of spectral response, appropriate standards were rarely available and each cell was therefore calibrated in the laboratory following each experiment.

The R.A.E. method of calibrating a solar cell[6] is based on the fact that the air-mass-zero short circuit current of a cell can be computed from a knowledge of the cell's relative spectral response in light of known intensity and spectral composition and Johnson's[7] curve for air-mass-zero sunlight. The

theory for the method is illustrated in Fig.3. In the case of the laboratory calibration the source used was a water filtered 3200°K tungsten iodine lamp.

The relative spectral response of all cells was measured from 0.35 to 1.15 μ at 0.05 μ intervals with a Hilger Watts D285 fused silica prism monochromator, fed from a 650 W, 3200°K tungsten-iodine lamp. The slits of the monochromator were fixed at 0.5 mm, and the intensity in each waveband measured with a compensated Schwarz vacuum thermocouple.

4.2 Electron irradiation

Following the assessment of initial performance, 4 covered thin cells, type RSC/2A and 4 covered thin cells, type WRC/2A were sequentially irradiated by 10^{13}, 10^{14}, 10^{15} and 10^{16} electrons cm^{-2} at 1 MeV using a Van de Graff accelerator. Three covered 12 mil 10 ohm cm - type RSC/2C cells were included in the study with a view to obtaining a comparison of the post-irradiation end-of-life performances, of the thick and thin covered cells. In a further experiment six 10 ohm cm thin cells and six 1 ohm cm thin cells were sequentially irradiated for fluences up to 10^{17} electrons cm^{-2} at 1 MeV aimed at comparing end-of-life performances for the two base resistivities.

The cells were mounted horizontally on a water-cooled 16 cm diameter aluminium block and enclosed in a vacuum chamber under a 125 micron aluminium diaphragm. During irradiation, the vacuum chamber was maintained under a vacuum better than 10^{-3} torr and the beam intensity was continuously monitored by means of a graphite Faraday Cup (1 cm^2 aperture) located in the centre of the water-cooled aluminium target block. The output from the Faraday Cup was fed to a chart recorder via a vibrating reed electrometer, to facilitate the determination of electron fluence while the timing circuit for the chart recorder was controlled by a Geiger counter facing the target beam and situated in a cable access slit in the wall of the target room. The mean beam intensity throughout the experiment was approximately 5×10^{10} electrons cm^{-2} sec^{-1}. The electron beam from the accelerator tube in the generator was scanned electromagnetically and this, combined with air scatter of the emergent beam, gave a beam uniformity better than ±5 per cent over the target area - as determined by mapping the target area with a small Faraday Cup in conjunction with a closed-circuit T.V. observation facility.

After each stage of the irradiation, the performance measurements described in section 4.1 were repeated.

4.3 Proton irradiation

Following the assessment of initial cell performance three matched batches of 1 x 2 cm 10 ohm cm n on p cells were formed. Each batch was comprised of 4, 12 mil cells and 6, 4 mil cells. These batches were sequentially irradiated by 70, 100 and 140 MeV protons for fluences up to 3.7×10^{12} protons cm^{-2} using a Synchrocyclotron. The cells were mounted in a perspex holder one behind the other; energy degradation being negligible for the number of samples used. Beam uniformity (better than 10%) and alignment were checked by a photographic film positioned behind the cell stack and fluence was determined by means of a Faraday Cup. The dose rate was 3×10^{7} protons cm^{-2} sec^{-1} and the overall accuracy of the dosimetry was ±10%. In addition to this experiment 4 thin 1 x 2 cm 10 ohm cm cells, were mounted on an aluminium jig, positioned in the 5 MeV proton window of a tandem Van de Graff accelerator and irradiated sequentially for fluences up to 2×10^{12} protons cm^{-2}. The beam uniformity was within ±5% and the dose rate was 1.7×10^{8} protons cm^{-2} sec^{-1}.

The problem of low energy 'synchronous altitude' proton irradiation of cells with exposed bar and back contacts and the protection afforded by various forms of coatings was studied by irradiating cells with 10^{13} 500 KeV protons cm^{-2} generated by a Van de Graff accelerator fitted with an electrostatic analyser. This dose is equivalent to 'synchronous altitude' proton irradiation for approximately one year and is sufficient to reveal significant changes in cell performance. The various modes of irradiations, cell types and configurations are depicted in the inset diagrams of Figs.10-17. Beam uniformity of ±3% over a one inch diameter circle in the proton exit window restricted the number of cells per irradiation to two 1 x 2 cm cells or one 2 x 2 cm cell. The dosimetry was based on a Faraday Cup calibration. The more important parameter in this experiment was the energy resolution, which was determined as being better than ±25 keV. The dose rate was 1.7×10^{10} protons cm^{-2} sec^{-1}.

4.4 Contact corrosion

This investigation was initiated by American reports, that under certain conditions of temperature and humidity, titanium-silver contacts on the satellite cells failed. These reports indicated that the cement used to fix the cover glass to the cell, may also influence the contact failure.

While Ferranti and R.A.E. Space Department have had limited experience of the storage-corrosion behaviour of Ti-Ag contacts, confined to occasional

American samples - they have been aware of the potential corrosion problem and have undertaken periodic measurements on a batch of 6, covered and 6, uncovered cells from the first batch of cells supplied for the British Ariel 3 satellite project in November 1965. These cells, which embodied a solderless plated contact system consisting of a composite layer of nickel copper and gold, were calibrated in Malta sunlight in June 1966 and again in July 1968. No special storage precautions were taken; thus these cells were exposed to ambient temperature and humidity 25°C, 60-80% relative humidity at the Royal Aircraft Establishment, Farnborough, England for nearly three years and were exposed to marine atmosphere in Malta for a total duration of 28 days.

In a study of the relative corrosion behaviour of Ti-Ag contacts and the standard Ferranti plated contacts, a series of environmental tests were devised to establish possible failure characteristics in each type of contact.

The batches of cells used were selected from standard Ferranti production cells, and from the thin cell development programme.

The cells tested were as follows:

(1) Bare cells.

(2) Bare cells which had the contact regions but not grid lines tinned with 60:40 tin lead solder.

(3) Bare cells, fitted with a 0.006inch glass micro sheet cover, which was cemented to the active surface of the cell using Silooloid 601 cement.

(4) Cells tinned as in (2) and also fitted with a glass cover as in (3).

(5) Bare cells with Ti-Ag contacts over-plated with copper.

The cells were tested under six conditions. Two are those in which the cell may be used in practice. The conditions were as follows:

(a) Room temperature and humidity.

The cells were laid in individual compartments on trays, and identity maintained throughout the experiment. The trays were stored in normal factory temperature and humidity, which ranges from 20°C-25°C and 45%-55% relative humidity.

(b) Room temperature and high humidity

The cells were laid on trays, and these were placed in an enclosed cabinet, in which there were open water troughs. This maintained a constant high humidity of not less than 90%.

(c) 50°C and high humidity

A thermostatically controlled oven was used which had open water troughs on the bottom shelf. The cells were laid in trays on the second shelf, using the top shelf to protect the cells from condensation.

(d) 50°C water immersion

Beakers of deionised water were placed in the 50°C oven. The cells were loaded into jigs and immersed in the water. Individual identity was maintained throughout the experiment.

(e) 100°C water immersion

Glass beakers were filled with deionised water and placed on a hot plate, whose temperature was controlled so that the water was just boiling. The cells were placed in jigs to maintain identity.

(f) 30°C and 100% relative humidity.

(g) 50°C and 100% relative humidity, this test being sequential to (f).

A thermostatically controlled humidity cabinet was employed at the Ministry of Technology's Electrical Inspection Establishment. No attempt was made to shield the cells from precipitation or condensation.

Performance measurements were made on the cells initially and following each test.

5 RESULTS AND DISCUSSION

5.1 Performance of thin cells from pilot production

The performance spread of the various types of thin cells described are shown in terms of voltage-current characteristics in Figs.4-6. The air-mass-zero efficiency values were calculated on the basis of total cell area (2 x 2 cm) rather than on 'active' cell area.

It may be noted that the 'uncovered' cell performance need not be compromised by the use of CeO_2 which reduces performance 'cover-loss' to a negligible extent. The pre- and post-cover performance curves of Figs.10-16

illustrate this fact while the curves for covered and uncovered cells in Figs.17 and 18 point to the high cover losses incurred by the use of grown SiO_2 coatings. Fig.5 indicates that performance of cells with evaporated Ti-Ag contacts and of those with plated Ni-Cu-Au contacts are much the same.

While the increased active area of the wrap-round cells (Fig.6) gives rise to a higher short circuit current value, these cells exhibit a softer voltage-current characteristic on account of their inherent higher series resistance. Thus cells with wrap-round contacts have much the same maximum power output as those with conventional contacts. The overriding factor in favour of the wrap-round cells is likely to be concerned with ease of assembling and repairing large arrays of these cells. It may be seen from Fig.6 that by increasing the boron doping level of the base silicon to correspond to 1 ohm cm resistivity, the increase in open circuit voltage and improved 'hardness' of the 'voltage-current' characteristics give rise to a considerable improvement in performance. The inherent danger of using 1 ohm cm p-type silicon is that it is much more susceptible to irradiation damage than 10 ohm cm p-type silicon. This result confirms experience with thick cells.

The overall yields from silicon slice starts to good physical and electrical cells quoted in Figs.4-6 are considered satisfactory for a pilot production exercise of this type. It was encouraging to find that no difficulty was experienced in handling the thin cells.

It is also interesting to note that only three thin cells were broken at the R.A.E. during their environmental studies on more than one thousand thin cells.

5.2 Electron irradiation

Fig.7 illustrates how the higher initial power output of a thick cell degrades more rapidly than for a thin cell during 1 MeV electron irradiation until, for fluences beyond 10^{15} electrons cm^{-2}, the power outputs are the same, notwithstanding the fourfold advantage of the thin cell in terms of power-to-weight ratio.

It is gratifying to note that the power degradation curve for the 12 mil cells (Fig.7) is in good agreement with the results obtained for Ferranti cells by Cherry and Statler[8], recently in the U.S.A.

These workers observed that the European 10 ohm cm cells were more radiation resistant than U.S. 10 ohm cm cells, thus to reach the same maximum power level as the equivalent U.S. cell at 10^{15} electrons cm^{-2}, the European cells had to be subjected to more than twice this dose. The reason for this behaviour almost certainly lies in the impurity content, particularly oxygen, of the silicon used. It is significant that all Ferranti cells are made from 'float-zone' crystals rather than 'pulled' crystals in spite of the increased raw material cost, and therefore have a lower oxygen content (two orders of magnitude) than American cells which to-date have been made predominantly from 'pulled' crystals.

The greatest susceptibility of 1 ohm cm p-type silicon to electron damage than 10 ohm cm p-type silicon is borne out by the results of Fig.8 where, despite a high initial performance the 1 ohm cm cells have a lower end-of-life performance than the 10 ohm cm cells for electron fluences exceeding 1.4×10^{15} electrons cm^{-2}. Thus for a 25% degradation of power output the 10 ohm cm cells will withstand 4.4 times the dose for the 1 ohm cm cells. This behaviour is controlled by the value of $f(E_t - E_f)$ in equation (1). For heavily doped n or p-type silicon, $f(E_t - E_f)$ is approximately unity but becomes a sensitive function of resistivity as E_f approaches E_t.

5.3 Proton irradiation

Fig.9 illustrates the performance equivalence of both thick and thin cells following high energy proton irradiation of uncovered cells.

It is evident that the proton damage coefficient increases rapidly for the lower proton energies, the 5 MeV proton irradiation being by far the most damaging in this experiment. For a 25% degradation of power output, the uncovered thin cells have to sustain relative doses of 13, 26 and 19 times more for the 70, 100 and 140 MeV protons respectively, than for the 5 MeV protons. In practice low energy proton damage may be obviated by using appropriate cover slips. These characteristics will be of considerable value in making a prognosis for a solar array's end-of-life performance following long term transfer orbits through the Van Allen Radiation Belts.

The results of the low energy (~500 keV) proton irradiation of cells with bar and back contacts exposed and also with various forms of shielding are shown in Figs.10-17. Figs.10, 11, 12 and 17 present data for cells with plated Ni-Cu-Au contacts while the remainder are concerned with cells having

Ti-Ag contacts. It may be seen from Figs.10 and 13 that irradiation of the bare bar contacts does not represent a serious problem. There is a small, but significant degradation of open circuit voltage (V_{oc}) and current in the vicinity of maximum power point indicative of junction damage especially in the case of the cells with plated contacts. This is believed to result from irradiation of the small margin of bare silicon around the bar contact and is supported by the fact that complete protection by cover glass cement obviates the problem (curves A, B Fig.11) whereas contact tinning with solder is not necessarily effective (curve D, Fig.11). The problem can, of course, be conveniently avoided by using a completely covered wrap-round cell (Fig.17) or bar contact brought out to the edges of the cell and complete cover glass coverage up to the inner edge of the contact.

Irradiation of the exposed back contact can have serious consequences; thus while the cells with Ni-Cu-Au contacts withstood this mode of irradiation (Fig.12) four cells with Ti-Ag contacts exhibited a serious collapse of their voltage-current characteristic. The reason for this difference in behaviour is that the 5 μ Ni-Cu-Au contacts are thick enough to prevent 500 keV proton penetration whereas many of the Ti-Ag contacts are not. Standard Ferranti Ni-Cu-Au contacts are produced to a 6-10 micron thickness specification. Using the 'Bragg Kleeman Rule' the mean range of 500 keV protons in copper and silver is 2.3 ±0.4 and 2.6 ±0.4 microns respectively. All of the cells showing voltage current (V-I) collapse had Ti-Ag back contacts between 2.2 and 1.3 microns thick. The V-I collapse is believed to result from high carrier compensation in the p-type silicon underlying the positive back contact which is thereby rendered non-ohmic.

Fig.16 illustrates the possible forms of protection for this type of cell when employed on a thin flexible solar array. In this respect it is interesting to note that irradiation of the exposed back surface of a wrap-round cell which also has its p-n junction exposed on this surface, produces a significant but not catastrophic softening of the V-I characteristic (Fig.17) and a small fall in open circuit voltage. The junction region on this type of cell must be shielded in any thin flexible array using this type of cell.

5.4 Contact corrosion

The voltage current characteristics of both a covered and uncovered Ariel 3 solar cell from the first batch of cells of this type to be supplied

to the Royal Aircraft Establishment in November 1965 are shown in Fig.18. The cells concerned are typical of six uncovered and six covered cells with solderless Ferranti Ni-Cu-Au contacts, selected for storage degradation observations. These cells were calibrated in Malta in June 1966 and in July 1968; the performance characteristics have remained invariant with time despite being exposed to ambient temperatures and humidity at the R.A.E. Farnborough for nearly 3 years and to a marine atmosphere in Malta for a total of 28 days.

The retention of their solderability has enabled these early cells to be used recently without any cleaning operation, to study interconnection and assembly techniques for large flexible arrays prior to the supply of thin cells. More than a thousand old Ariel 3 cells have been used for this purpose; moreover, a 48 cell patch of these cells with soldered invar interconnects has withstood 2000 thermal cycles between -120°C and +80°C. This patch has also been held at -160°C for 10 hours. No interconnect failures or contact failures were experienced. Similarly the R.A.E. are assembling thermal sensor diodes for the Black Arrow X3 satellite solar cell experiment employing precisely the same contacts and soldering technology developed for large flexible array assembly. These devices have withstood 1000 cycles between -120 and +80°C and maintained at -160°C for 10 hours.

In contrast to the foregoing experience, the R.A.E. have received several American cells with solderless Ti-Ag contacts which have tarnished to such an extent that they were rendered unusable within a year. Another one year old cell lost its complete back contact while being demounted from low strength sticky tape.

The results of the corrosion tests (e) to (g) described previously are presented in Tables 1-4.

The definition of cell contact failure used in the programme was the amount of deterioration of the squareness of the voltage current characteristic. The squareness was measured as $I_{SC} - I_{400}$. Where I_{SC} - short circuit current, I_{400} - current at the load point of 400 mV. A 2 x 1 cm cell was defined to have failed when the $I_{SC} - I_{400}$ value increased by at least 5 mA above the initial value.

Both contact systems are seen to be stable at temperatures up to 25°C and humidities up to 90% relative humidity for periods up to 3000 hours.

This conclusion applies to cells in the bare, bar contact tinned, covered and uncovered contact tinned conditions. No deterioration effects attributable to the covering cement were detected.

When the temperature is raised to 50°C and combined with high humidity, contact deterioration can be observed. Plated cells were shown to withstand this condition for periods up to 2800 hours, without failure in all conditions of tinning and covering. The titanium-silver cells showed serious failure rates after exposure to these conditions exceeding 300 hours. The extent of failure after 300 hours appears to be reduced but not eliminated by either tinning the exposed titanium-silver contacts or applying a cemented cover glass. For exposure periods below 300 hours the titanium-silver contact system is stable.

When extreme conditions are employed, such as water immersion at 50°C or 100°C, the superior behaviour pattern of the plated cells at high temperature and humidity is reversed. The plated contacts either tinned or untinned suffer rapid failure in water immersion tests. At 50°C 100% cell failure occurs within 400 hours, and at 100°C the effect is accelerated to 18 hours. Again applying tinning to the contacts only slows down the effect slightly, and does not eliminate it.

When cells with untinned Ti-Ag contacts are exposed to direct precipitation and condensation in saturated atmospheres of 100% relative humidity they fail rapidly (less than 672 hours) even at 30°C whereas for the same conditions untinned plated Ni-Cu-Au contacts and Ti-Ag contacts over-plated with Cu-Au withstand the test. If the temperature for this test is increased to 50°C however, 75% of the plated contacts fail after a further exposure of 672 hours while the Ti-Ag contacts over-plated with Cu-Au withstand even this extreme test.

All of the preceding results may be considered in the light of three corrosion mechanisms characterised by the degree of dampness of the corroding surface[9].

(a) Dry atmospheric or chemical corrosion due to the presence of SO_2-H_2S trace impurities.

(b) Moist atmospheric corrosion associated with 'capillary condensation' under dust or in micropores for relative humidities less than 100% relative humidity.

(c) Wet atmospheric corrosion for 100% relative humidity corresponding to exposure to direct precipitation/immersion.

The differences observed between the tests involving a very thin layer of electrolyte on the surface of the contacts (moist corrosion) and those involving complete immersion of the contacts in an electrolyte (wet corrosion) are very marked since in the former case corrosion proceeds via local micro-cells and benefits from localised protection by corrosion products.

The differences observed in the behaviour of the various type of cell contacts may be explained as follows.

Since the Ti-Ag contacts are produced by evaporation of the 2 metals through a mask the resultant metallised contact will be a sharply defined 'sandwich' of the 2 metals when viewed in cross section. Thus, both metals will be exposed to humidity. The standard Ferranti Ni-Cu-Au plated contacts however, will have each layer of metal completely shrouded by the following metal i.e. the only metal which would be exposed to humidity and other corrosion conditions would be gold.

Furthermore a study of electrode potential shows that the potential produced between titanium and silver should produce corrosion of the titanium when directly exposed to high humidity conditions, whereas even if the nickel-copper of the Ferranti system were exposed together to a 'corrosive atmosphere' the electrode potential of the two metals are almost perfectly matched and this should exhibit no corrosive attack.

This would explain the better corrosion resistance of the plated contacts over the conventional Ti-Ag contact system. It was also shown that tin dipping and overplating of titanium-silver contacts produced corrosion resistant cells. This would indicate that the exposed couple of titanium and silver metal has been protected by a 'shrouding' mechanism such that the adverse electrode potentials of the two metals cannot give rise to corrosion.

6 CONCLUSIONS

(1) Thin cells can be made using production techniques with good performance characteristics and satisfactory yields.

(2) Results of high energy electron and proton irradiation studies demonstrate the greater radiation resistant properties of thin cells.

(3) Low energy proton irradiation of cells with plated Ni-Cu-Au contacts and Ti-Ag contacts have established that irradiation of covered cells with bare bar and back contacts do not present a serious problem for contact thicknesses in excess of the mean proton range in the contact. It is necessary to ensure that no active cell area is exposed around the cover glass or bar contacts to preclude junction damage and hence open circuit voltage degradation.

(4) Contact corrosion studies have established that:

(a) Ti-Ag contacts require either tinning with solder or overplating with copper to obviate chemical-dry atmospheric-corrosion.

(b) Standard Ferranti Ni-Cu-Au contacts are adequately resistant to both dry and moist atmospheric corrosion and need no special storage precautions or tinning.

ACKNOWLEDGEMENTS

The authors wish to thank the Director of the Central Research and Engineering Division, British Insulated Callenders' Cables Ltd., for the provision of the 1 MeV electron irradiation facility and the Director of the United Kingdom Atomic Energy Authority, Harwell for the provision of the proton irradiation facilities. They also wish to thank their colleagues at the Royal Aircraft Establishment, Farnborough and Ferranti Ltd., Chadderton for assistance in the experimental work.

Table 1

PERCENTAGE FAILURES OF NICKEL COPPER GOLD PLATED AND Ti-Ag CONTACTS IN CONDITIONS a, b AND c

Cell description	Condition	Time of exposure (h)			
		336	730	1128	2856
Ni-Cu-Au untinned uncovered	a	0	0	0	0
	b	0	0	0	0
	c	0	0	0	0
		288	2016		
Ni-Cu-Au tinned uncovered	c	0	0		
		72	216	360	
Ti-Ag-Cu untinned uncovered	c	0	0	0	

Table 2

PERCENTAGE FAILURE OF NICKEL COPPER GOLD PLATED CONTACTS TINNED AND UNTINNED AND Ti-Ag CONTACTS UNDER CONDITION d

Cell description	Condition	Time of exposure (h)					
		284	48	96	120	264	384
Ni-Cu-Au untinned uncovered	d	0	0	0	0	30%	100%
		288	2016				
Ni-Cu-Au tinned uncovered	d	0	80%				
		24	48	192	312	456	
Ti-Ag-Cu untinned uncovered	d	0	0	0	0	0	

Table 3

PERCENTAGE FAILURE OF NICKEL COPPER GOLD PLATED CONTACTS TINNED AND UNTINNED, AND Ti-Ag CONTACTS UNDER CONDITIONS e

Cell description	Condition	Time of exposure (h)						
Ni-Cu-Au untinned uncovered	e	5 70%	12 80%	18½ 100%	24½ 100%			
Ni-Cu-Au second untinned uncovered	e	7 0	14 36%	19 60%	26 80%	32 88%		
Ni-Cu-Au tinned uncovered	e	12 30%	18 40%	24½ 40%	31½ 60%	41½ 90%	48 90%	
Ti-Ag untinned uncovered	e	7 0	14 100%					
Ti-Ag-Cu untinned uncovered	e	4½ 0	10½ 0	17½ 0	31½ 0	38 0	45 0	49 0

Table 4

PERCENTAGE FAILURES OF NICKEL COPPER GOLD, Ti-Ag AND Ti-Au OVERPLATED WITH Cu-Au

Cell description	Condition	Time of exposure
		672 h
Ti-Ag untinned uncovered	f	100%
	g	100%
Ti-Ag-Cu-Au plated uncovered	f	0
	g	0
Ni-Cu-Au untinned uncovered	f	0
	g	75%

g sequential to f

REFERENCES

No.	Author	Title, etc.
1	R. L. Crabb F. C. Treble	Thin silicon solar cells for large flexible arrays. Nature, 29 March 1967, Sciences et Industries Spatiale 11/12 (1967)
2	W. Cherry et al.	Sixth Photovoltaic Specialist Conference - U.S.A. April 1967 - Seminar Session
3	-	Editorial, Implion News (U.S.A.) Vol. 1, No. 1 (1968)
4	R. N. Hall W. Shockley W. T. Read	Physical Review, Vol. 87, p. 387 and 385 (1952)
5	M. W. Walkden	The spectral energy distribution of sunlight in Malta. R.A.E. Technical Report 67248 (1967)
6	F. C. Treble	Solar cell performance measurement. Fourth International Symposium on Batteries (1964)
7	F. S. Johnson	The solar constant. Journal of Met. Vol. 2, No. 6 (1954)
8	W. R. Cherry R. L. Statler	Photovoltaic properties of U.S. and European silicon cells under 1 MeV electron irradiation. Goddard Space Flight Centre Preprint X-716-68-204 (1968)
9	N. D. Tomashov	Theory of corrosion and protection of metals. Macmillan (1966)

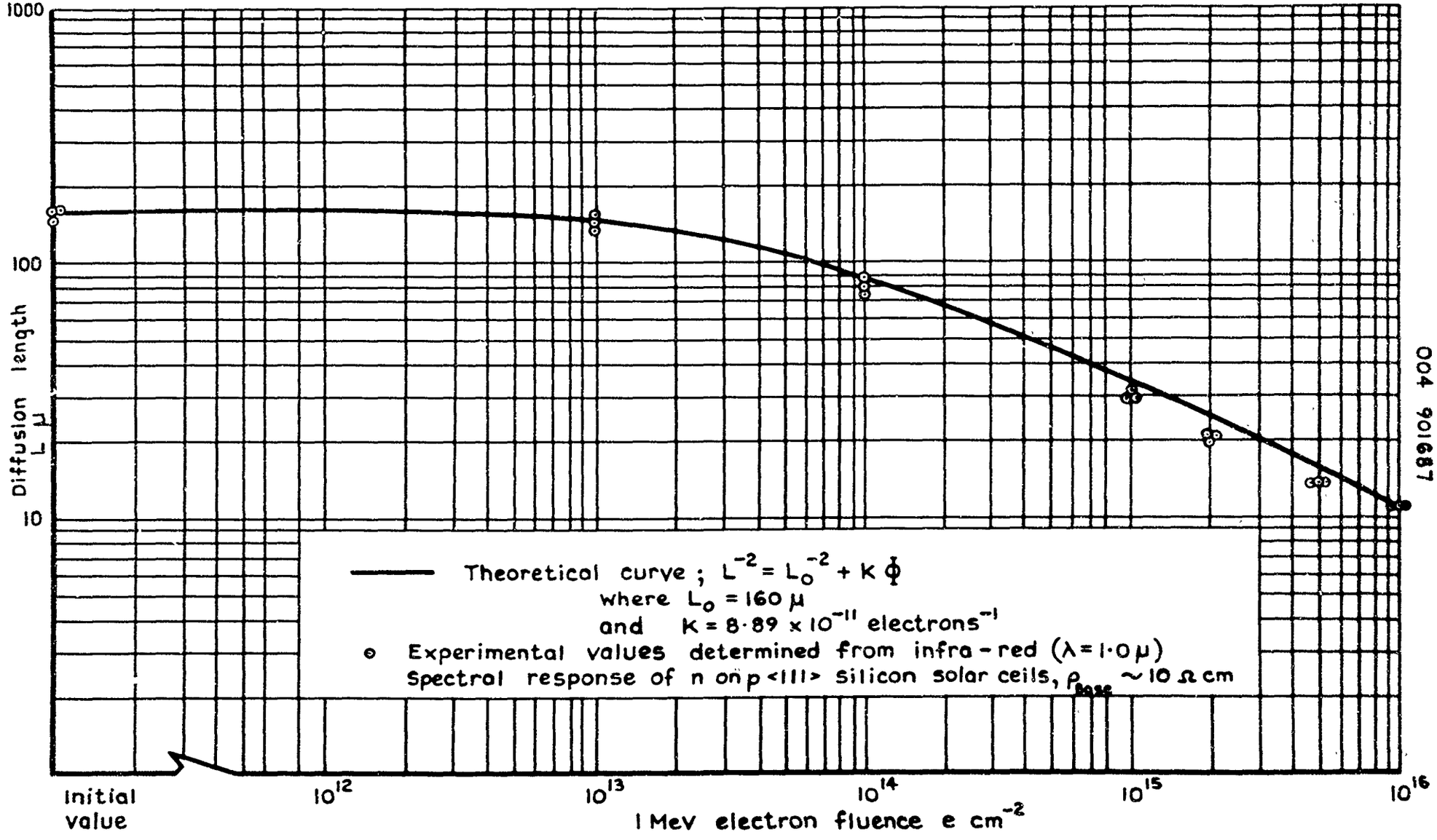

Fig.1 Minority carrier diffusion length degradation of electron irradiated 10 ohm-cm P-type silicon

Fig.1

Fig. 2

004 901688

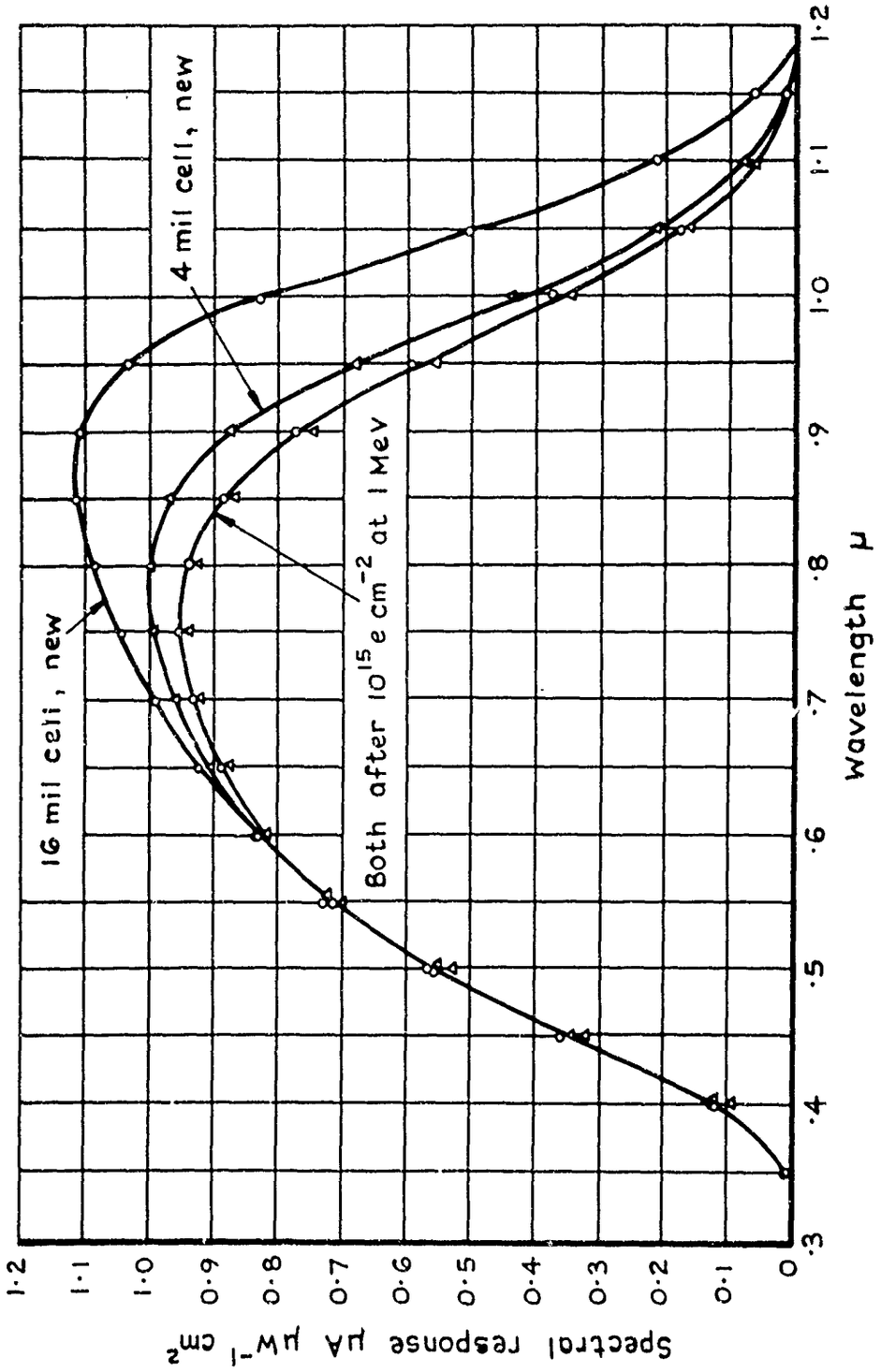

Fig. 2 Spectral response of electron irradiated 4 and 16 mil thick silicon solar cells

Fig. 3

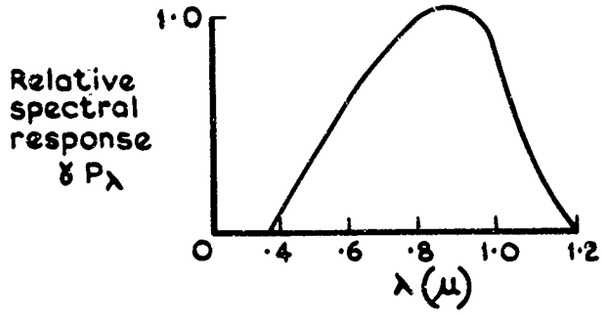

Curve A rel spectral response of cell

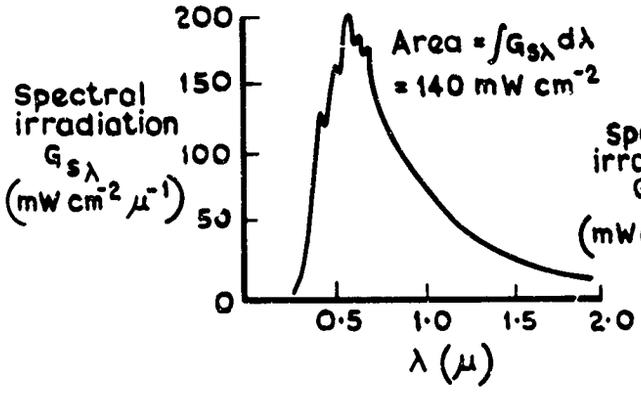

Curve S air mass O sunlight

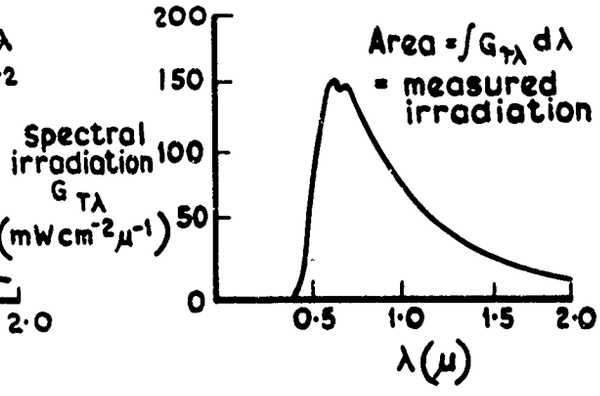

Curve T calibration source

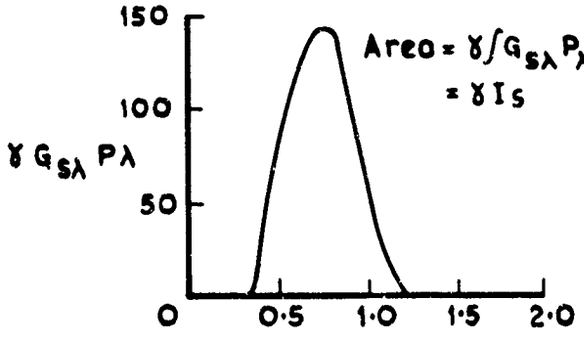

Curve (A X S)

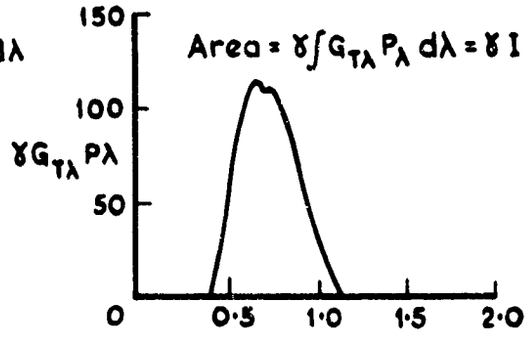

Curve (A X T)

$$I_S = I_T \frac{\int G_{S\lambda} P_\lambda d\lambda}{\int G_{T\lambda} P_\lambda d\lambda}$$

Fig. 3 Theory of air - mass - zero short circuit current prediction

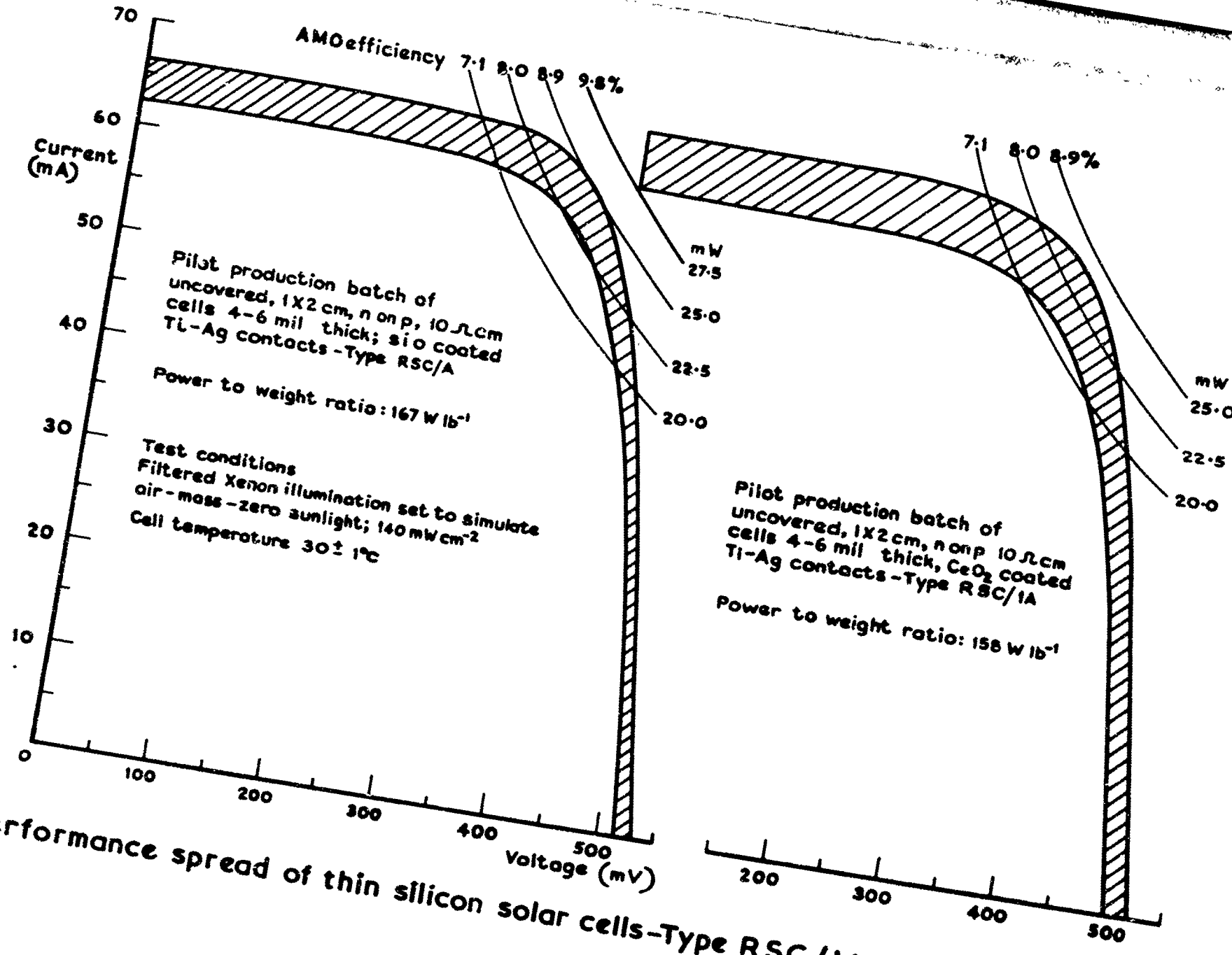

Fig.4 Performance spread of thin silicon solar cells-Type RSC/1A- from pilot production

004 901690

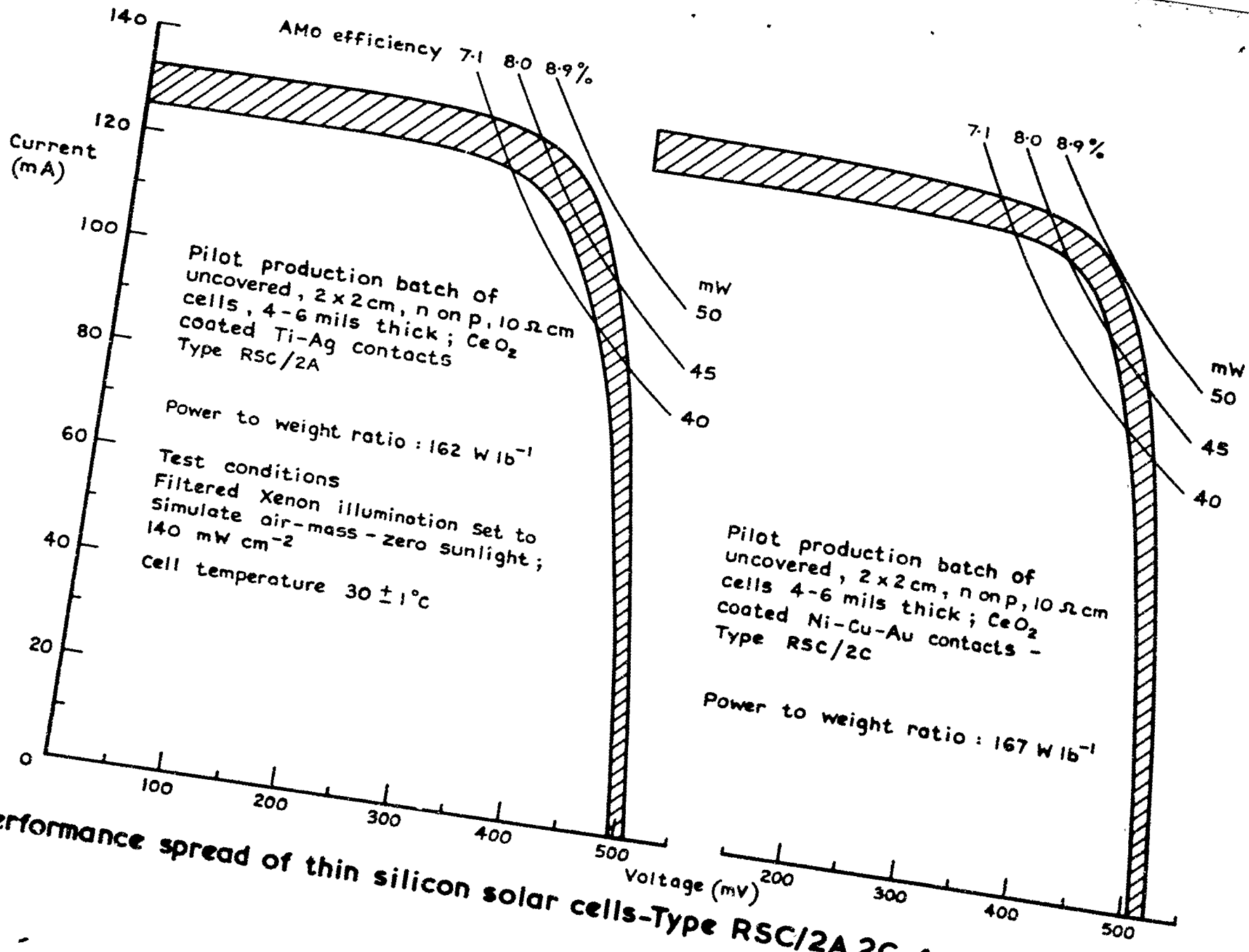

Fig. 5 Performance spread of thin silicon solar cells-Type RSC/2A,2C from pilot production

Fig. 5

004 901691

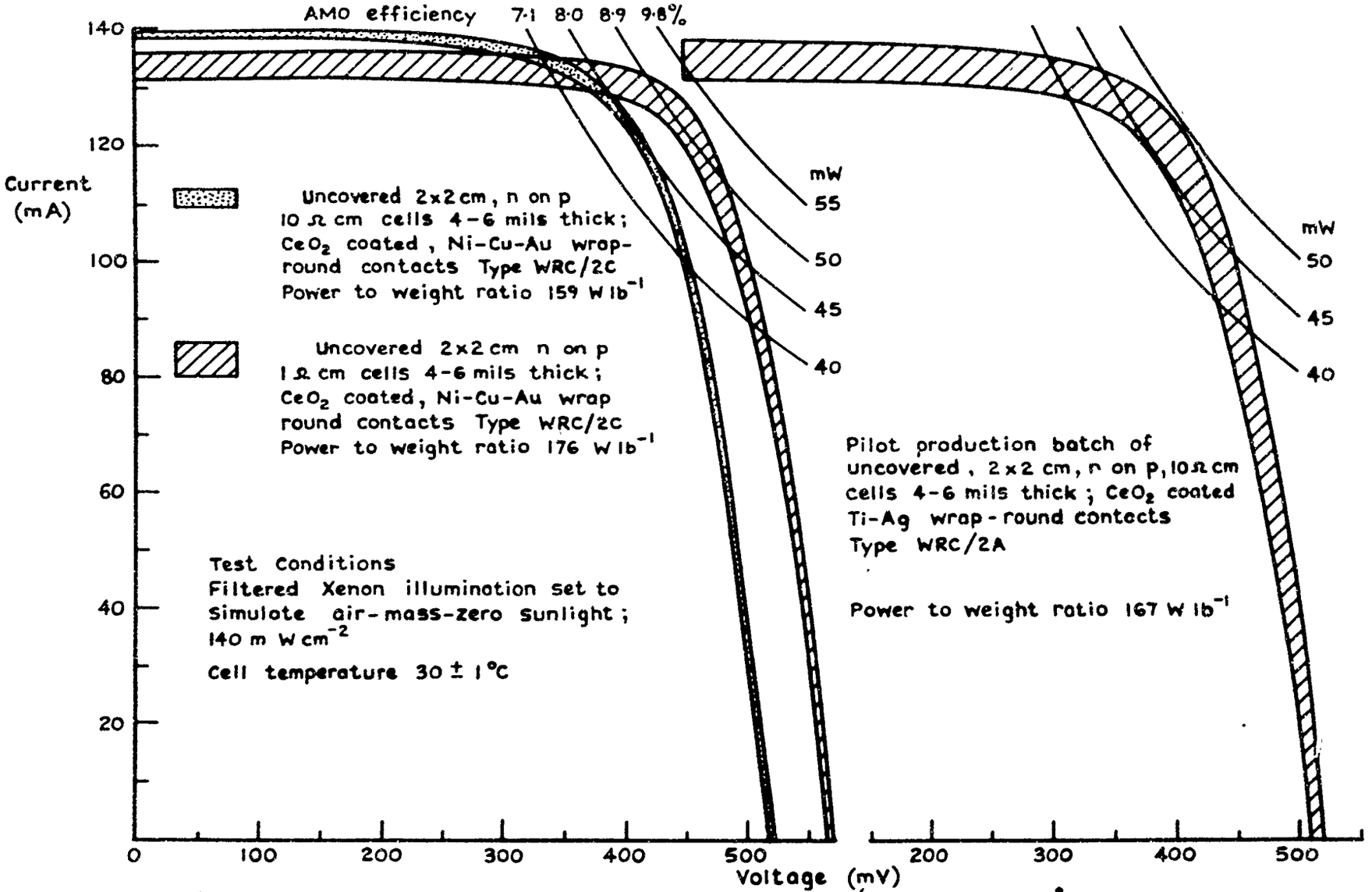

Fig. 6 Performance spread of thin silicon 'wrap round' solar cells - Type WRC/2C,2A-from pilot production

004 901692

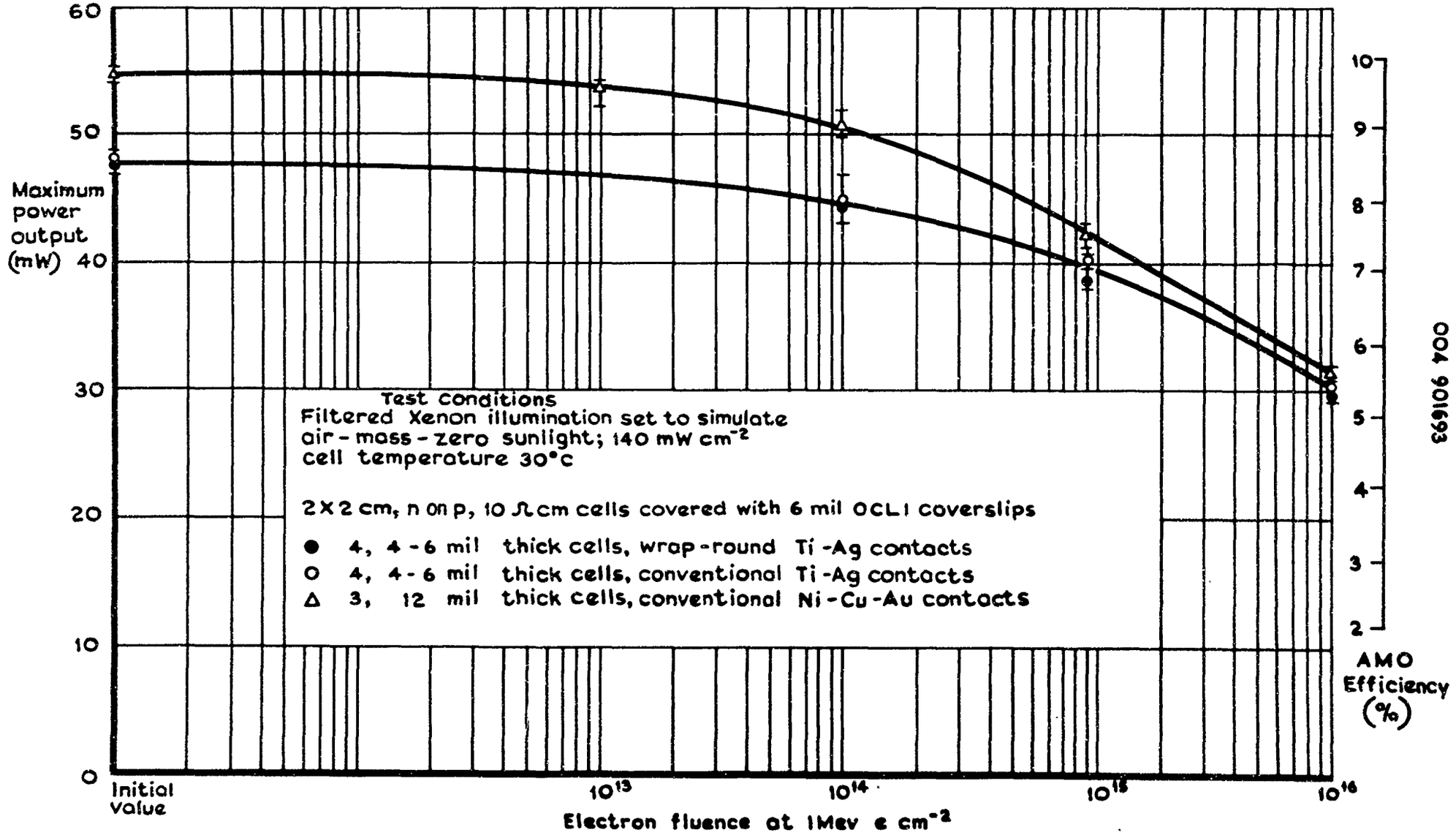

Fig.7 Power output of electron irradiated covered 4 and 12 mil silicon solar cells

Fig.7

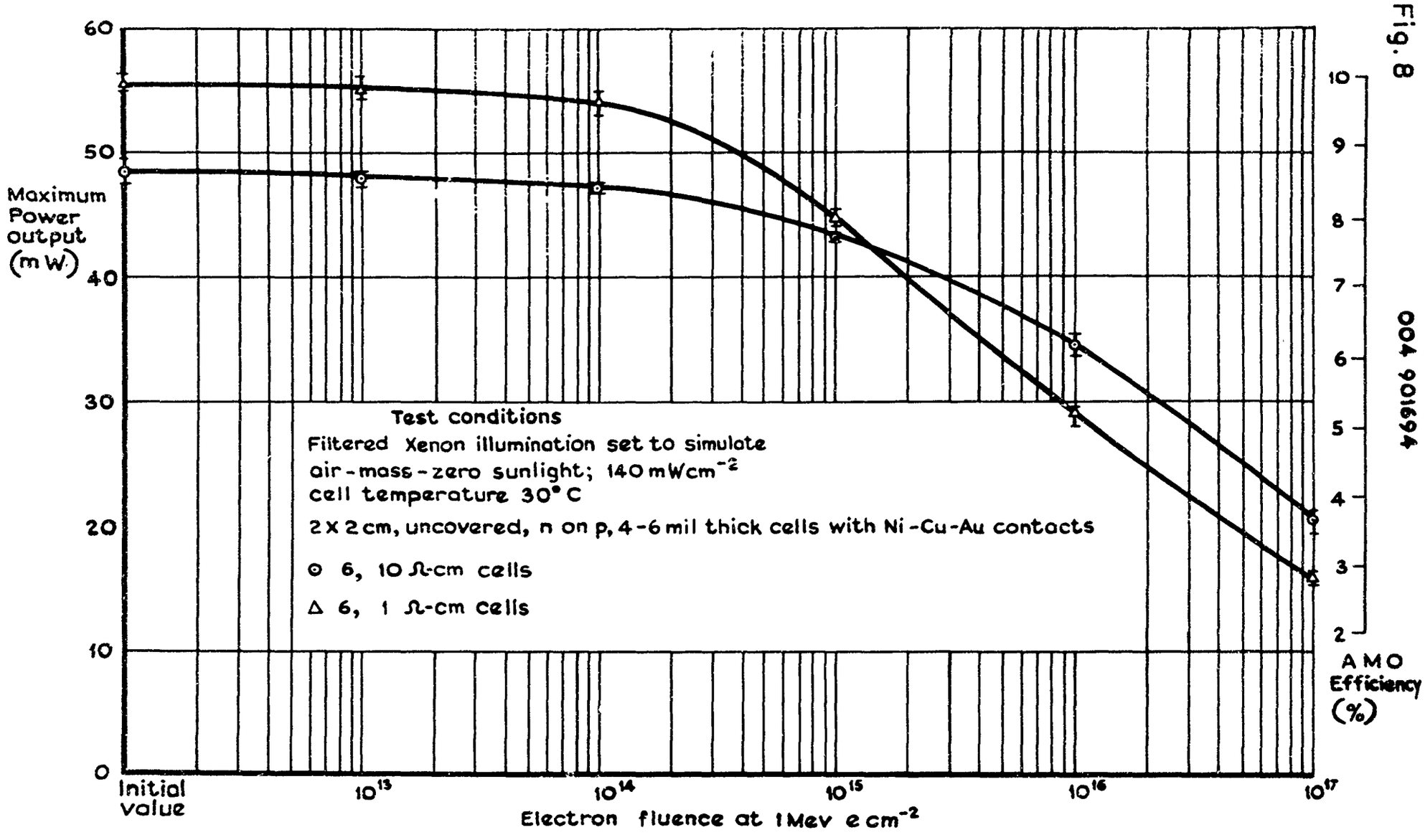

Fig.8 Power output of electron irradiated, 1 and 10 Ω cm thin silicon solar cells

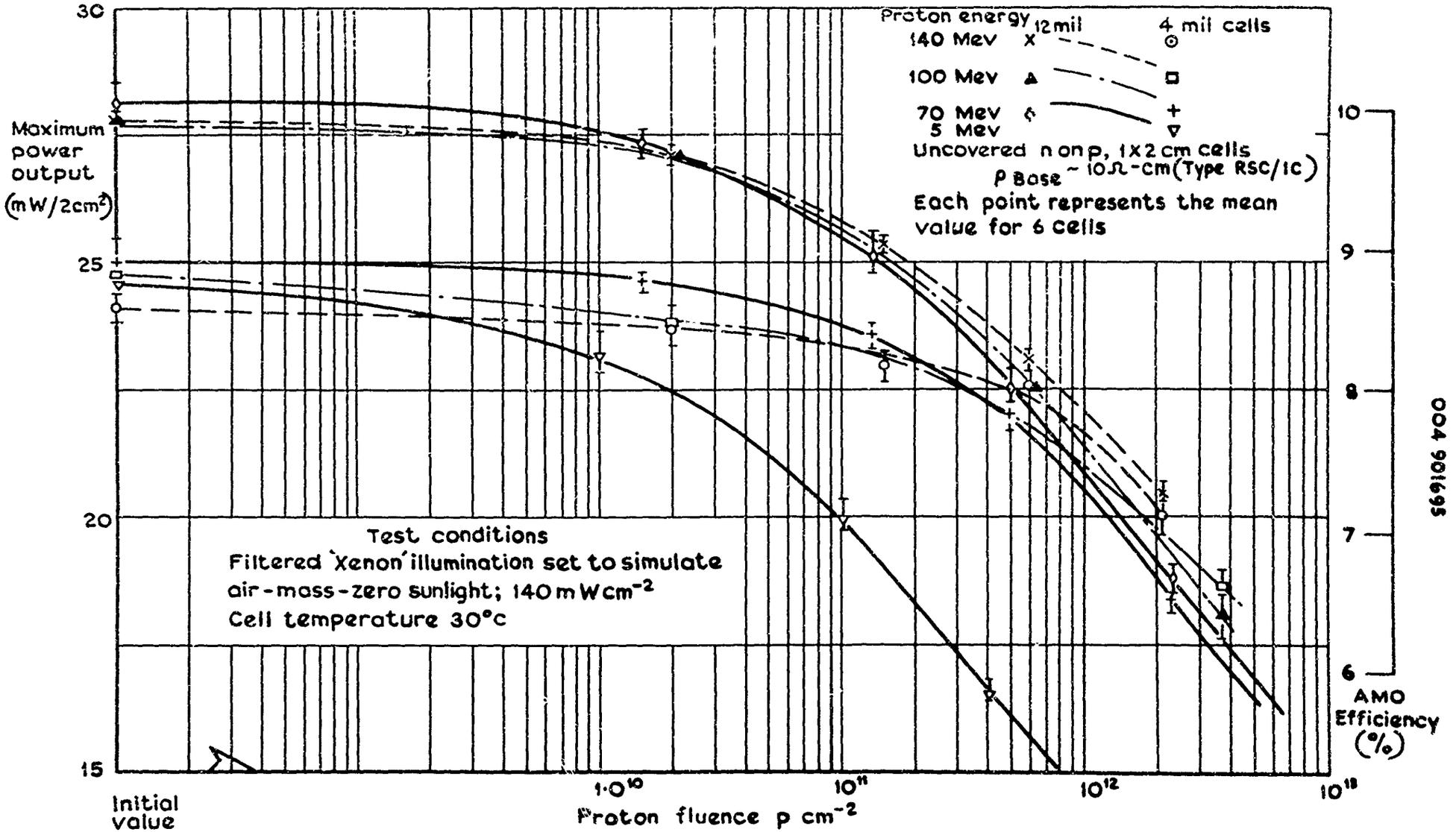

Fig.9 Power output of proton irradiated, 4 and 12 mil thick silicon solar cells

004 901695

Fig. 9

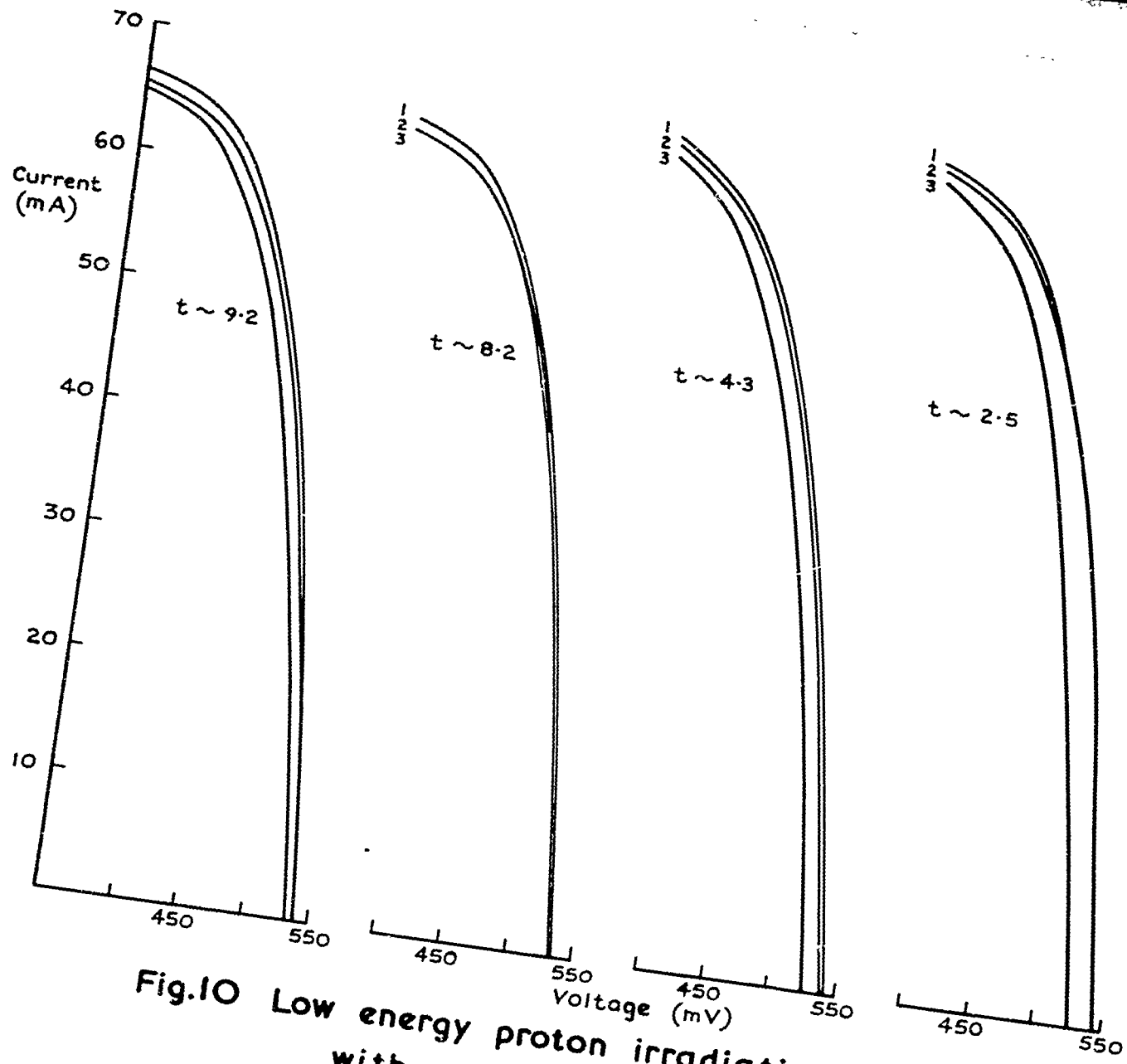

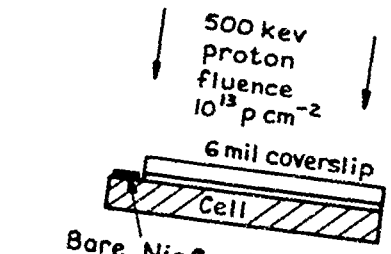

12 mil, 1 x 2 cm, n on P, 10 Ω-cm cells

1 Pre-cover performance
2 Post-cover performance
3 Post-irradiation performance

Simulated AMO sunlight -filtered Xenon

Cell temp 30 ± 1°C

004 901696

Fig. 10

Fig.10 Low energy proton irradiation of covered solar cells with exposed Ni-Cu-Au, 'bar' contacts

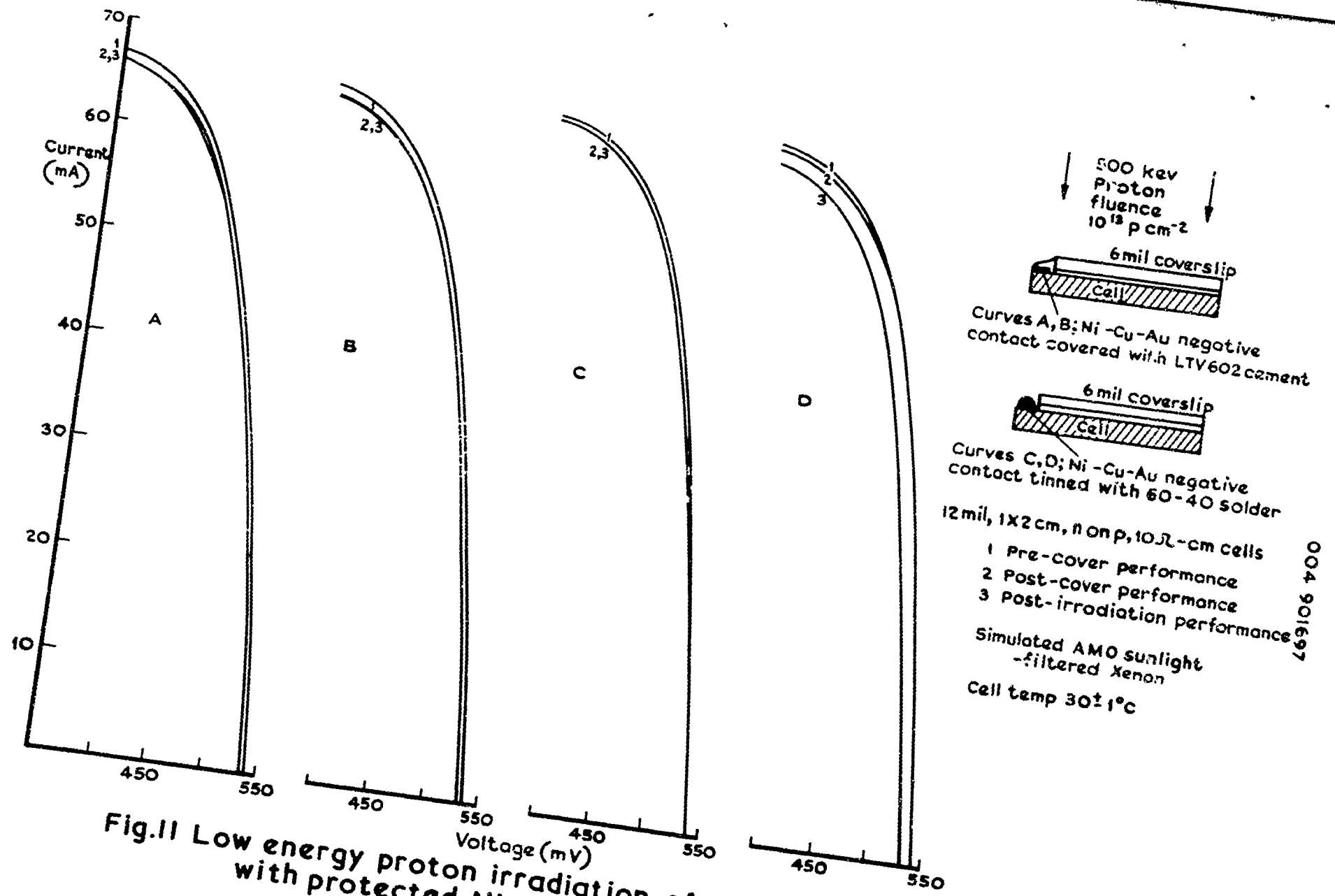

Fig.11 Low energy proton irradiation of covered solar cells with protected Ni - Cu - Au - 'bar' contacts

Fig.11

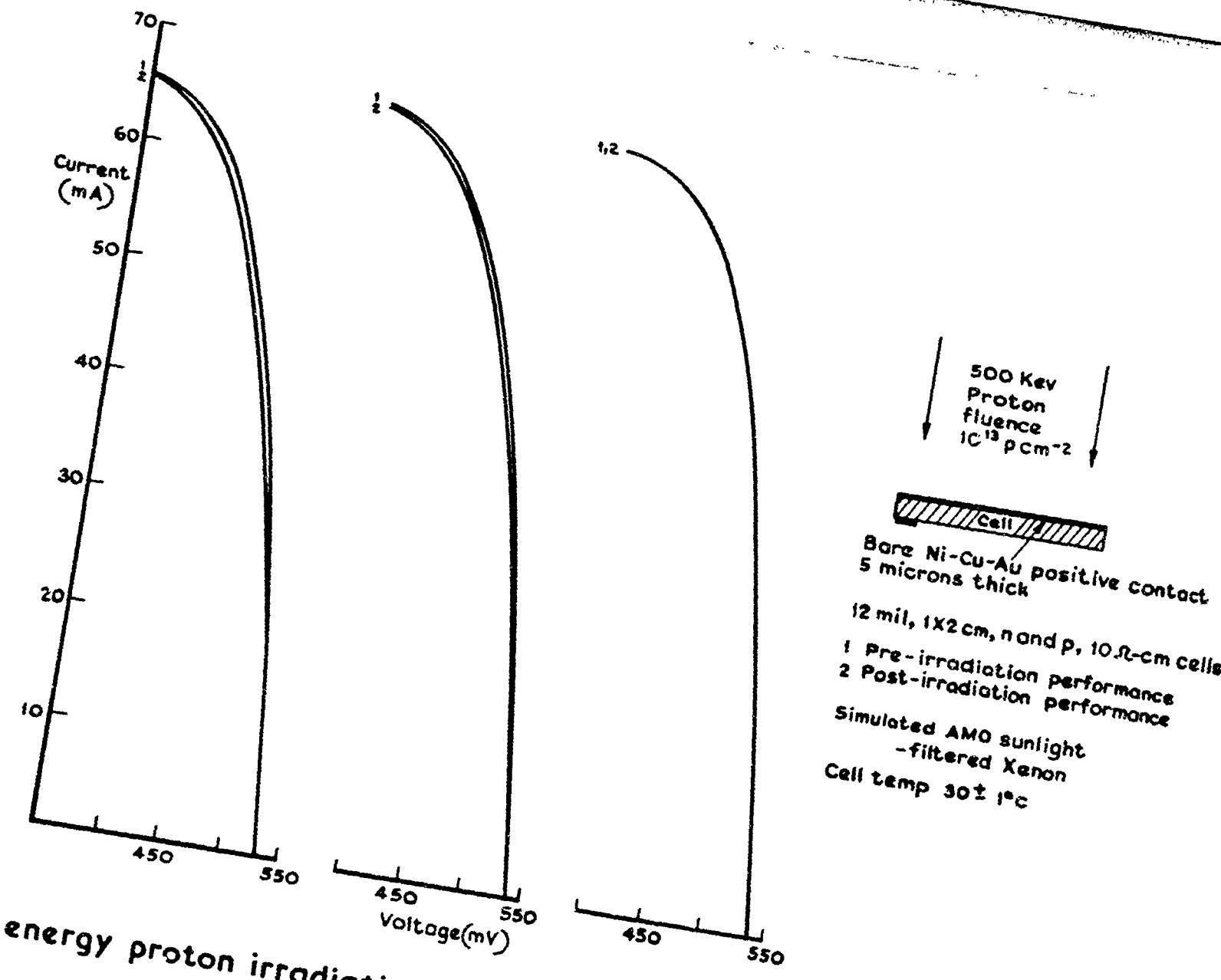

Fig. 12

Fig. 12 Low energy proton irradiation of solar cells with exposed Ni-Cu-Au back contacts

004 90198

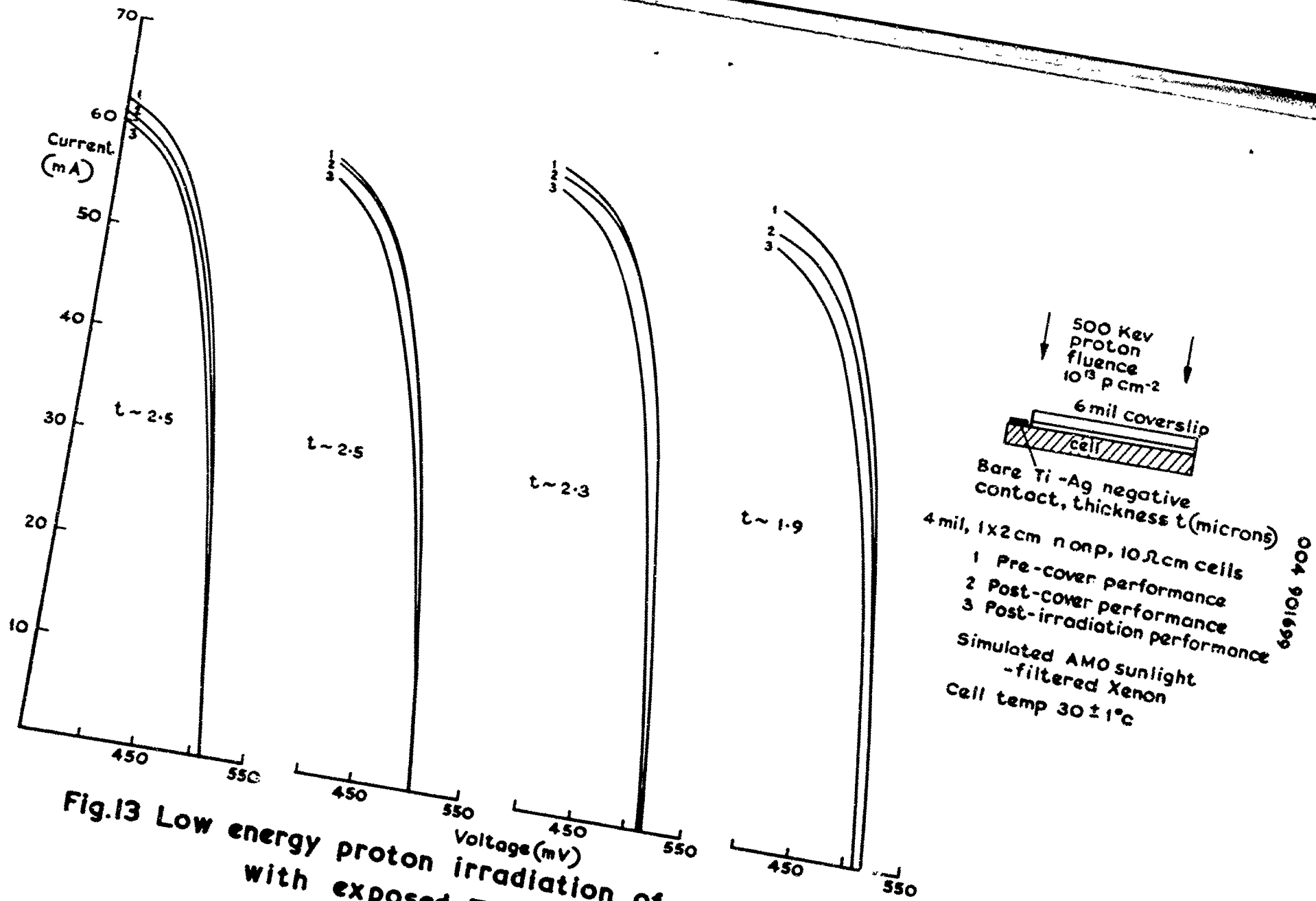

Fig.13 Low energy proton irradiation of covered solar cells with exposed Ti-Ag 'bar' contacts

Fig. 13

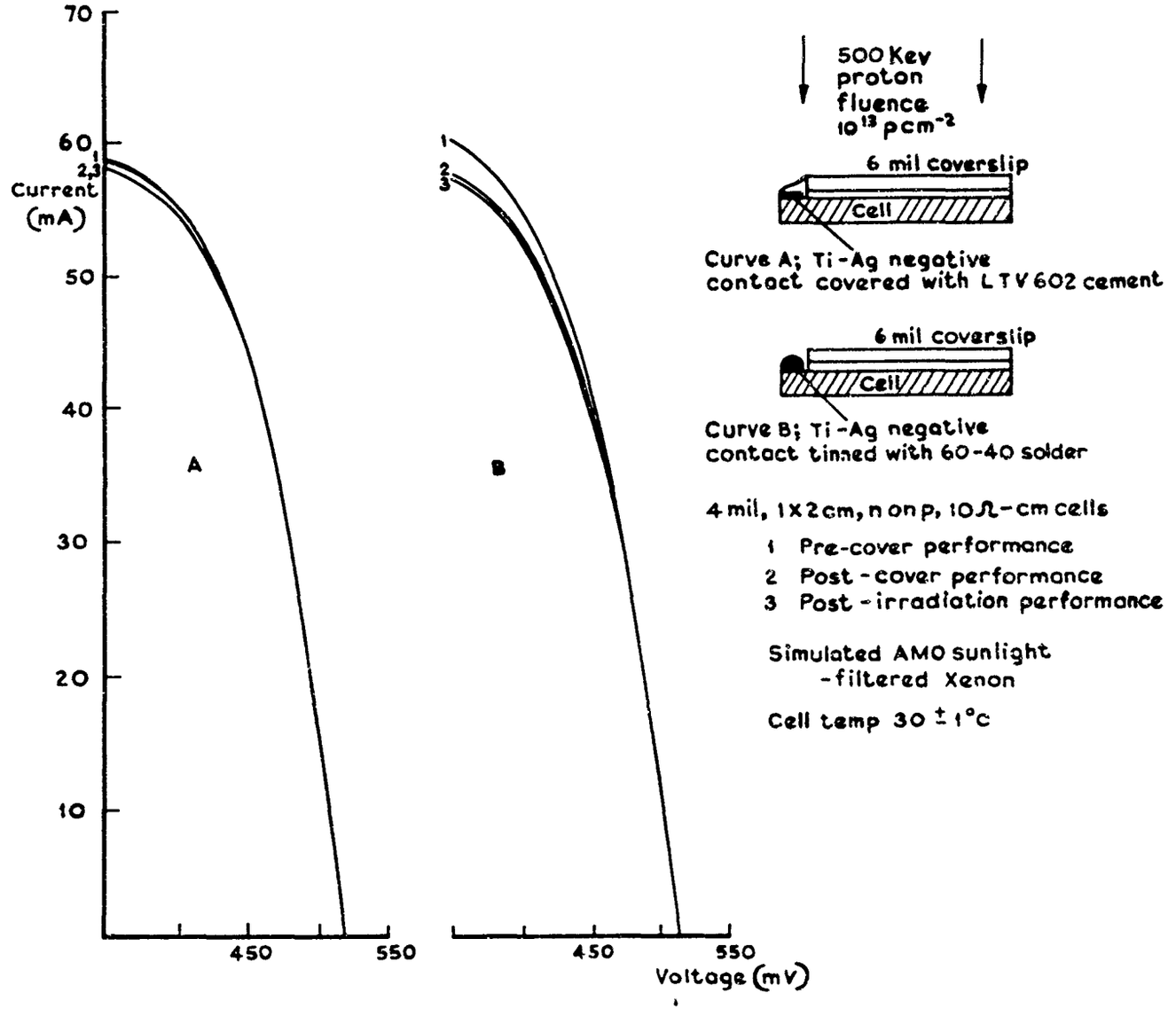

Fig.14 Low energy proton irradiation of covered solar cells with protected Ti-Ag 'bar' contacts

004 901700

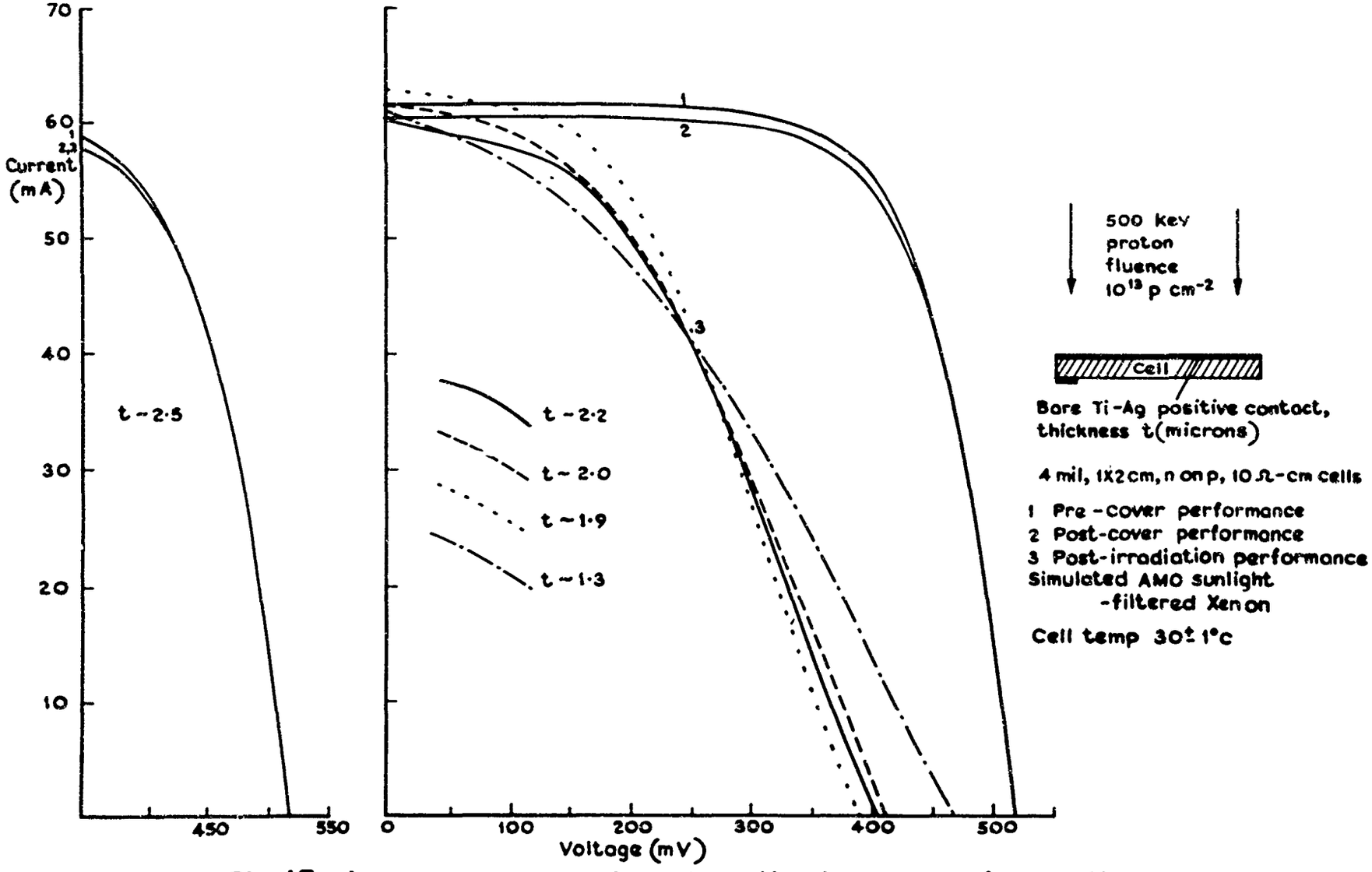

Fig.15 Low energy proton irradiation of solar cells with exposed Ti-Ag 'back' contacts

004 901701

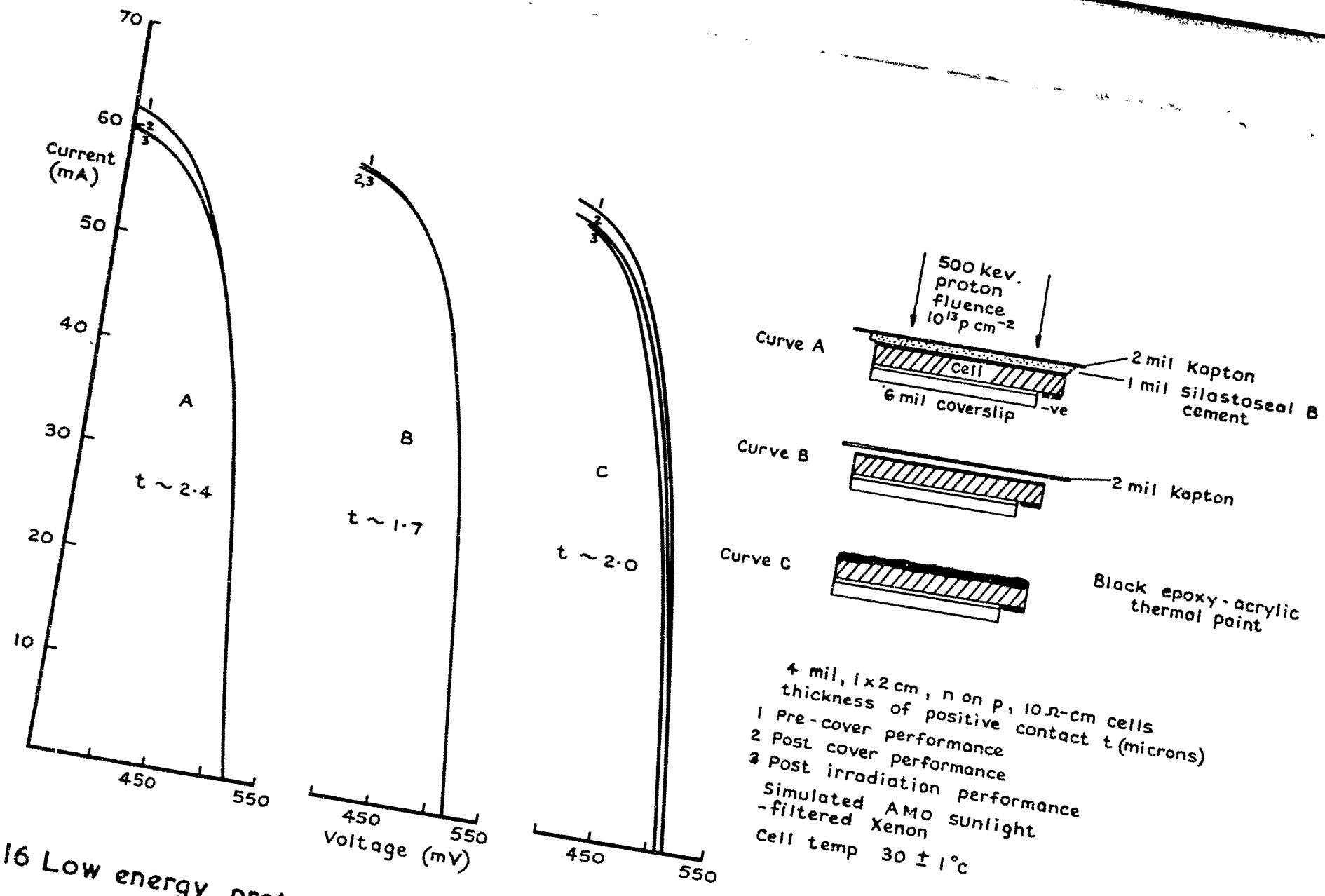

Fig.16

004 901702

Fig.16 Low energy proton irradiation of solar cells with protected Ti–Ag 'back' contacts

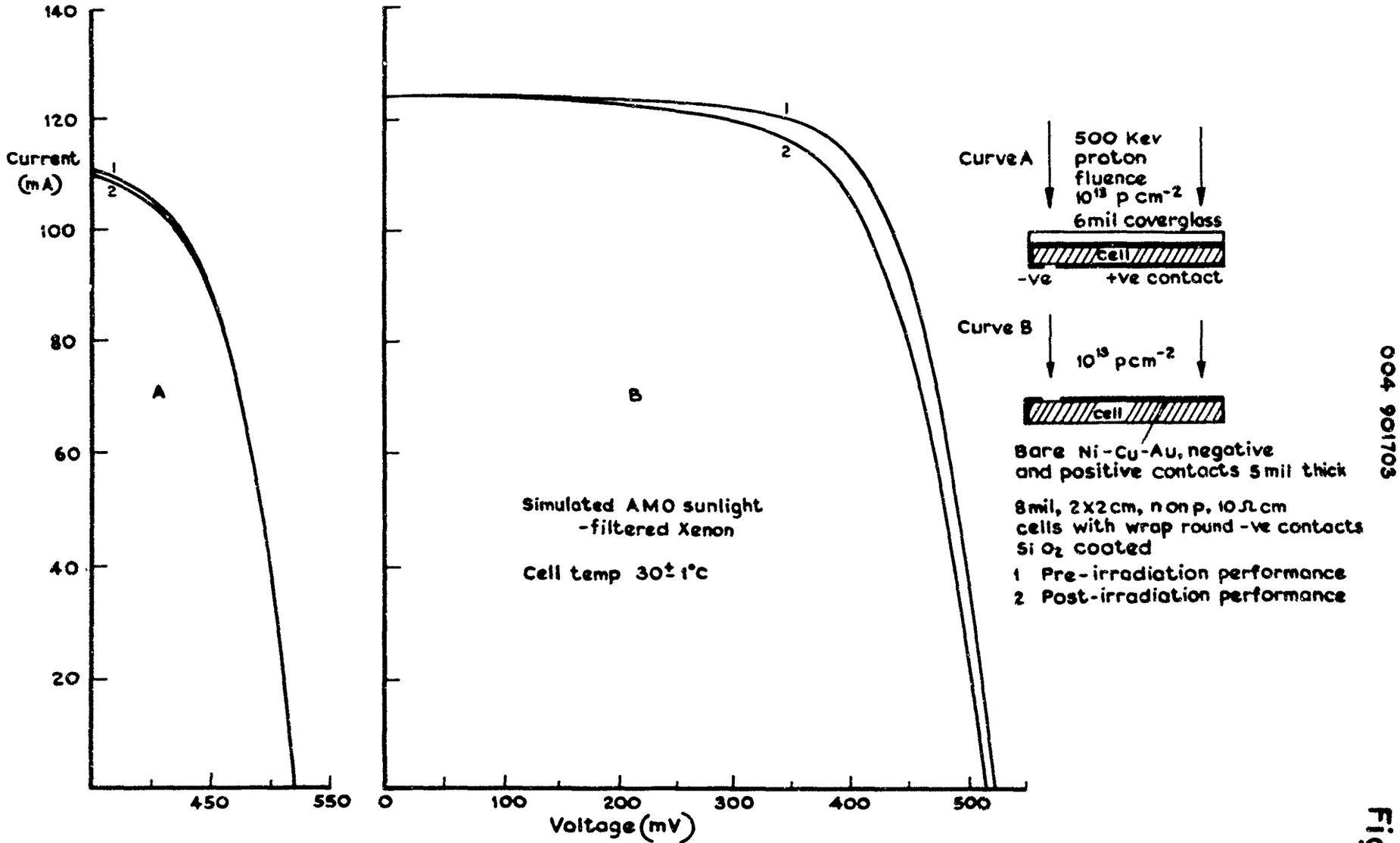

Fig.17 Low energy proton irradiation of 'wrap-round' solar cells

Fig.17

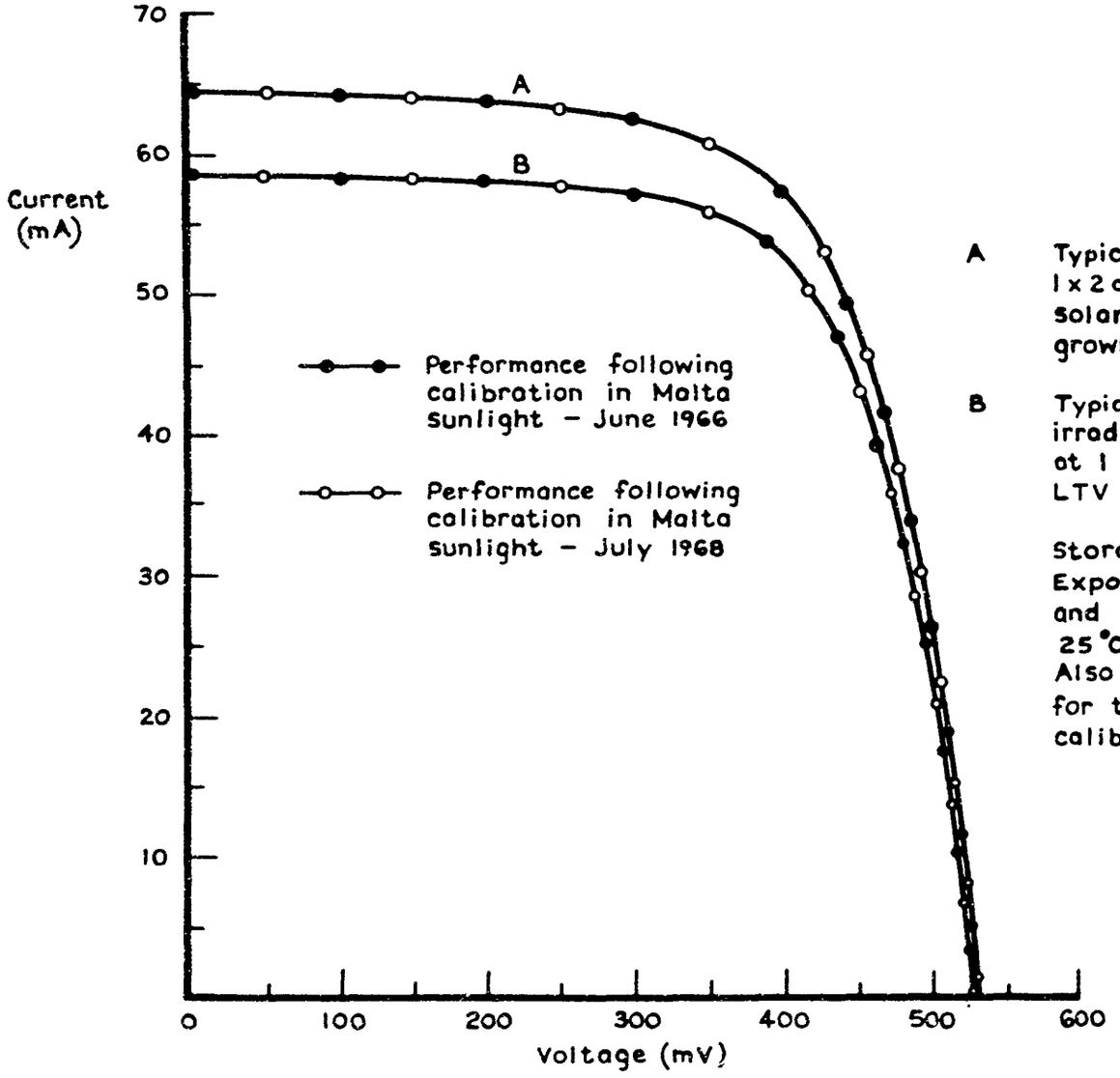

A Typical uncovered 'Ariel 3', Ferranti 1 x 2 cm, 16 mil, n on p, 10 Ω cm solar cell; Ni-Cu-Au contacts, grown SiO_2 antireflection coating

B Typical covered 'Ariel 3', cell irradiated with 10^{13} electrons cm^{-2} at 1 MeV. Coverslip affixed with LTV 602 cement

Storage conditions:-
Exposed to ambient temperature and humidity - R.A.E. Farnborough, England 25°C, 60-80% R.H. since November 1965. Also to Malta coastal atmosphere for two weeks-1966 and 1968, during calibration. No precautions taken

Fig. 18

004 901704

Fig.18 Performance of Ferranti 'Ariel 3' solar cells with Ni-Cu-Au contacts exposed to ambient temperature and humidity since November 1965